Hindawi Publishing Corporation
International Journal of Photoenergy
Volume 2016, Article ID 3058429, 9 pages
http://dx.doi.org/10.1155/2016/3058429

Research Article

Adsorption and Photocatalytic Kinetics of Visible-Light Response N-Doped TiO_2 Nanocatalyst for Indoor Acetaldehyde Removal under Dark and Light Conditions

Yu-Hao Lin,[1] Chih-Huang Weng,[2] Jing-Hua Tzeng,[3] and Yao-Tung Lin[3]

[1]*Centre for Environmental Restoration and Disaster Reduction, National Chung Hsing University, 250 Kuo-Kuang Road, Taichung 40227, Taiwan*
[2]*Department of Civil and Ecological Engineering, I-Shou University, Kaohsiung City 84008, Taiwan*
[3]*Department of Soil and Environmental Sciences, National Chung Hsing University, 250 Kuo-Kuang Road, Taichung 40227, Taiwan*

Correspondence should be addressed to Yao-Tung Lin; yaotung@nchu.edu.tw

Received 25 December 2015; Revised 16 March 2016; Accepted 6 April 2016

Academic Editor: Suresh C. Pillai

Understanding the removal nature of the indoor volatile organic compounds under realistic environment conditions would give clear guidance for the development of air purification devices. The study investigated the removal of indoor acetaldehyde using visible-light-responsive N-doped TiO_2 (N-TiO_2) photocatalyst under visible-light irradiation (light) and in the absence of light (dark). The adsorption kinetics of acetaldehyde onto N-TiO_2 followed a pseudo-second-order model. The magnitude of acetaldehyde adsorption is proportional to temperature, and the results were fitted to the Langmuir isotherm model. Moreover, the effect of initial acetaldehyde concentration and visible-light intensity on the photooxidation of acetaldehyde was well described by the Langmuir-Hinshelwood model. Results show that the mesoporous N-TiO_2 catalyst had a high ability to absorb acetaldehyde in the dark condition, and then acetaldehyde was subsequently photooxidized under visible-light irradiation. The adsorption capacity was found to increase with decreasing temperature. The negative value of ΔG° and the positive value of ΔS° indicate that the adsorption of acetaldehyde onto N-TiO_2 was a spontaneous process. Finally, a reaction scheme for removal process of indoor acetaldehyde by N-TiO_2 was proposed.

1. Introduction

Indoor volatile organic compounds (VOCs) and polycyclic aromatic hydrocarbons are especially serious for people who spend much of their time in airtight dwellings [1, 2]. Generally, there are two options to remove the VOCs: capture and destruction. Adsorption is one of the most reliable techniques to remove the VOCs in capture category. Adsorption process is classified into two types, that is, physical adsorption and chemical sorption, based on the interaction type between adsorbate and adsorbent [3]. In the destruction category, VOCs can be destroyed by various oxidation processes. The photocatalytic oxidation is one of the effective destruction techniques for the removal of VOCs [4]. As one of the major VOCs, acetaldehyde (CH_3CHO) has been frequently used as model compound for the indoor air contamination studies [5]; meanwhile, acetaldehyde can adversely affect the human cardiovascular system. Therefore, using photocatalytic technique to remove acetaldehyde is of considerable interest.

The uniform spreading of TiO_2 on a support medium is a means of increasing the photocatalytic reaction area for indoor air purification [6]. Ever since the coating of TiO_2 on fiberglass fibers could successfully remove indoor VOCs under UV-light illumination [7], self-cleaning paints or home appliances using photocatalysis over TiO_2-coated materials are beginning to be commercialized to remove indoor VOCs. Unfortunately, TiO_2 cannot function effectively when irradiated with fluorescent light and then cannot be widely applied to indoor use. Thus, expanding the range of applications of TiO_2 has been investigated through attempts

to increase the sensitivity of TiO_2 to visible light [8, 9]. Recently, visible-light-responsive TiO_2, such as nitrogen-doped TiO_2 (N-TiO_2) and N,S-codoped TiO_2, have been developed and successfully applied to oxidize a variety of VOCs completely to CO_2 under visible-light irradiation [10–14]. Efforts have also been made to explore the reaction kinetics and reaction intermediate of photocatalytic oxidation [15]. Various kinetic and environmental parameters, such as initial concentration, light intensity, and relative humidity, have been shown affecting the process of visible-light-responsive TiO_2 [16, 17]. A detailed study of the adsorption phenomena occurring on TiO_2 could provide useful insight into the understanding of the photodegradation reaction in the dark and light conditions. Bao et al. [18] and Venditti et al. [19] investigated the adsorption kinetic of a visible-light-active TiO_2 and the sequential photocatalyst photodegradation process of contaminants under visible-light irradiation and in the absence of light. However, the light intensity from the fluorescent light source in the indoor room only works approximately 10 hr in day time, and the indoor air often flows slowly.

The objective of this study is to investigate the adsorption and photooxidation kinetics of visible-light-responsive N-TiO_2 nanosized photocatalyst for indoor acetaldehyde removal under visible-light irradiation (light condition) and in the absence of light (dark condition). The influence of key parameters, such as initial acetaldehyde concentration, light intensity, and temperature, was investigated on the removal of acetaldehyde under simulated airtight environment.

2. Materials and Methods

2.1. Preparation and Characterization of N-TiO_2. The procedure for the synthesis of N-TiO_2 composite procedure was modified from literature [14, 20]. The precursors, ammonium hydroxide, titanium tetraisopropoxide, and absolute ethanol, were mixed under a 4°C water bath. After the hydrolysis and condensation reaction, colloid was centrifuged and then calcined at 500°C temperature to obtain the N-TiO_2 composite. Detailed synthesis of N-TiO_2 composite procedure refers to the literatures [14]. Size and morphological characterizations of N-TiO_2 were determined using a scanning electron microscope (SEM, S2700 Hitachi, Japan). The optical absorption responses of N-TiO_2 were obtained using UV-vis (Hitachi, U-3900H, Japan). The specific surface areas of N-TiO_2 were measured by the Brunauer-Emmett-Teller nitrogen absorption specific surface area (BET-N_2 SSA) method using a surface area analyzer (BET Micromeritics ASAP 2020, USA). The crystal phases of the N-TiO_2 were analyzed by XRD (PANalytical X'Pert Pro MRD, USA).

2.2. Adsorption and Photooxidation Kinetic Experiments. Kinetic experiments of acetaldehyde adsorption onto N-TiO_2 were performed to establish the effect of time on the adsorption process and to quantify the adsorption rate. Experiments were conducted with different temperatures (°C), initial acetaldehyde concentration (ppmv), and visible-light intensity (mW/cm^2). The sequential experimental procedure including dark and visible-light stages was as follows. Firstly, the catalyst dosage of 0.2 g N-TiO_2 was coated on the bottom of the reactor, and the desired concentration of acetaldehyde was injected into the reactor to conduct the absorption reaction without light irradiation (dark reaction). In the dark reaction, temperature was controlled at 5, 15, 25, 35, and 45°C by placing the reaction into the isothermal incubator. After reaching the thermal absorption equilibrium in the dark stage, the photooxidation experiment was sequentially implemented under the various light intensities and initial acetaldehyde concentrations. The visible-light illumination was provided by three-colored fluorescent lamps (March T5-8W/865, Taiwan), and the lamps combined with a cut-off filter ($k > 400$ nm) were vertically placed outside the reactor, above the center of the reactor. Illumination intensity was measured with a luminance meter (ILT1700, International Technologies, USA). The samples were withdrawn at designed time intervals and analyzed using a gas chromatograph (GC, PerkinElmer, Clarus 500, USA) equipped with a flame ionization detector (FID) and a thermal conductivity detector (TCD). Based on the pervious study [17], O_2 concentration can be neglected in the photooxidation when O_2 concentration is greater than 10%. Because the changes of O_2 concentration in indoor environment are not obvious, the impact of O_2 concentration on the pollutant removal was neglected.

2.3. Mathematical Models

2.3.1. Adsorption Kinetics. Adsorption isotherm experiments in the dark condition were performed to determine the maximum adsorption capacity and thermodynamic parameters. The amount of acetaldehyde adsorbed per unit mass of the adsorbent (q_t, in μmol/g) at time t (hr) was computed using the following expression:

$$q_t = \frac{(C_0 - C_t)V}{m}, \tag{1}$$

where C_0 (μmol/L) and C_t (μmol/L) are the acetaldehyde concentrations before and after adsorption, respectively, for time t (hr); m (g) is the amount of catalyst; and V is the volume (L) of the reactor. The kinetic data were analyzed using a pseudo-second-order (PSO) model, expressed as

$$\frac{dq_t}{dt} = \frac{1}{q_e} + k_2 (q_e - q_t)^2, \tag{2}$$

where q_e (μmol/g) denotes the amounts of acetaldehyde adsorbed on N-TiO_2 (μmol/g) at equilibrium, respectively, and k_2 is the PSO rate constant (g/μmol/hr). After integration of (2) and application of boundary conditions $q_t = 0$ at $t = 0$ and $q_t = q_t$ at $t = t$, the integrated form of the equation becomes

$$\frac{1}{q_e - q_t} = \frac{1}{q_e} + k_2 t \tag{3}$$

which can also be written as

$$\frac{t}{q_t} = \frac{1}{B} + \left(\frac{1}{q_e}\right) t \tag{4}$$

Table 1: Kinetic models for the acetaldehyde photooxidation by N-TiO_2.

Type	Model	Light intensity	Rate constant	Adsorption equilibrium constant K_{CH_3CHO}
I	L–H monomolecular	—	k	$\frac{K_aC_a}{1+K_aC_a}$
II	L–H light intensity-monomolecular	I^{α}	k'	$\frac{K_aC_a}{1+K_aC_a}$

I: light intensity (mW/cm^2); k: rate constant (μmole/hr); k': intrinsic rate constant (μmole/hr); α: order constant; K_a: adsorption equilibrium constant (1/ppmv); C_a: acetaldehyde concentration (ppmv).

in the linear form, where $B = k_2 {q_e}^2$ is the initial sorption rate as $t \to 0$. If the PSO kinetics is applicable, the plot of t/q_t versus t will show a linear relationship, which allows computation of q_e, k_2 (g/μmol/hr), and B without having to know any parameter beforehand.

Temperature effects on the adsorption of acetaldehyde were further investigated. The linear form of the Arrhenius equation is expressed as follows:

$$\ln(k_2) = \ln(A) - \frac{E_a}{RT}, \tag{5}$$

where A is the preexponential factor, R (J/mol-K) is the universal gas constant, T (K) is the absolute temperature, and E_a (kJ/mol) is the activation energy.

2.3.2. Adsorption Isotherms. The Langmuir adsorption isotherm was used to describe the acetaldehyde adsorption:

$$q_e = \frac{K_L C_e q_{\max}}{1 + K_L C_e}, \tag{6}$$

where q_e (μmol/g) is the amount of acetaldehyde adsorbed at equilibrium, K_L (L/mol) is the Langmuir adsorption constant, C_e (ppmv) is the acetaldehyde concentration at equilibrium, and $q_{\max}$ (μmol/g) is the maximum adsorption capacity. Equation (6) can be rearranged to

$$\frac{C_e}{q_e} = \frac{1}{K_L q_{\max}} + \left(\frac{1}{q_{\max}}\right) C_e. \tag{7}$$

From the plot of (C_e/q_e) versus C_e, the values of $q_{\max}$ and K_L are determined for the adsorption system.

2.3.3. Kinetics of Photooxidation. The kinetics of acetaldehyde photooxidation by N-TiO_2 was described by using the Langmuir-Hinshelwood (L-H) approach [6]. Based on the assumption of L-H model, the oxidative product of acetaldehyde (i.e., CO_2) did not influence the reaction rate. Equations for the dependence of kinetics on environmental variables, such as acetaldehyde concentration and light intensity, were obtained and shown in Table 1.

3. Results and Discussion

3.1. Characterization of N-TiO_2. Figure 1(a) shows the crystal phases of as-prepared N-TiO_2. The X-ray diffraction peaks marked with letters "A" correspond to the anatase phase. A major peak of 2 theta at 25.5° corresponds to crystal plane (101) of anatase. A higher peak intensity is indicative of stronger anatase crystallinity; thus, the synthesized N-TiO_2 would be expected to have high photoactivity. Figure 1(a) also shows the synthesized N-TiO_2 sample had typical peaks of polycrystalline anatase structure, but no dopant related peaks, such as TiN, which was possibly due to either the movement of dopant ions into interstitial positions of the TiO_2 structure or the ion concentration being too low to be detected [21]. Figures 1(b) and 1(c) show the surface morphology of N-TiO_2; the SEM measurement result indicates that single N-TiO_2 particle in agglomerates exhibited uniform spherical shape with a size range from 20 to 50 nm.

Figure 1(c) demonstrated that the N-TiO_2 exhibited a type IV isotherm and a type H_2 hysteresis loop at lower relative pressure region, which are typical characteristics of mesoporous structure with ink bottle pores. The hysteresis loop at lower relative pressure region ($0.4 < P/P_0 < 0.8$) and higher relative pressure ($0.8 < P/P_0 < 1.0$) was attributed to smaller mesopore and larger mesopores, respectively. The BET-N_2 SSA, pore size, and pore volume of N-TiO_2 catalyst are approximately 45.3 m^2/g, 6.9 nm, and 0.13 cm^3/g, respectively. Such heterogeneous-type pore is conducive to the adsorption of acetaldehyde. A comparison of optical absorption spectra of the N-TiO_2 and commercial TiO_2 (Degussa P25) samples was shown in Figure 1(d). The absorption at wavelengths shorter than 400 nm can be assigned to the intrinsic band gap absorption of TiO_2. The N-TiO_2 samples show a stronger absorption than that of P25 in the visible-light region (>400 nm) and a significant red shift of the absorption edge to a lower energy was observed. This result demonstrated that band gap narrowing has successfully been achieved by the doping of N into the TiO_2 lattice. Such visible-light absorption of the N-TiO_2 originated from the oxygen vacancy, N interstitial doping, and N substitution in the TiO_2 structure [14, 22, 23].

Figure 2 showed the acetaldehyde removal ability using N-TiO_2 photocatalyst under dark and light conditions. The photocatalyst was kept in the dark for at most 4 hr to reach the adsorption equilibrium at different starting acetaldehyde concentrations; this result should not be surprising because N-TiO_2 is a mesoporous material. As shown in the inset graph in Figure 2, while the acetaldehyde was gradually photooxidized with the light irradiation time, the concentration of CO_2 was simultaneously increased, indicating that

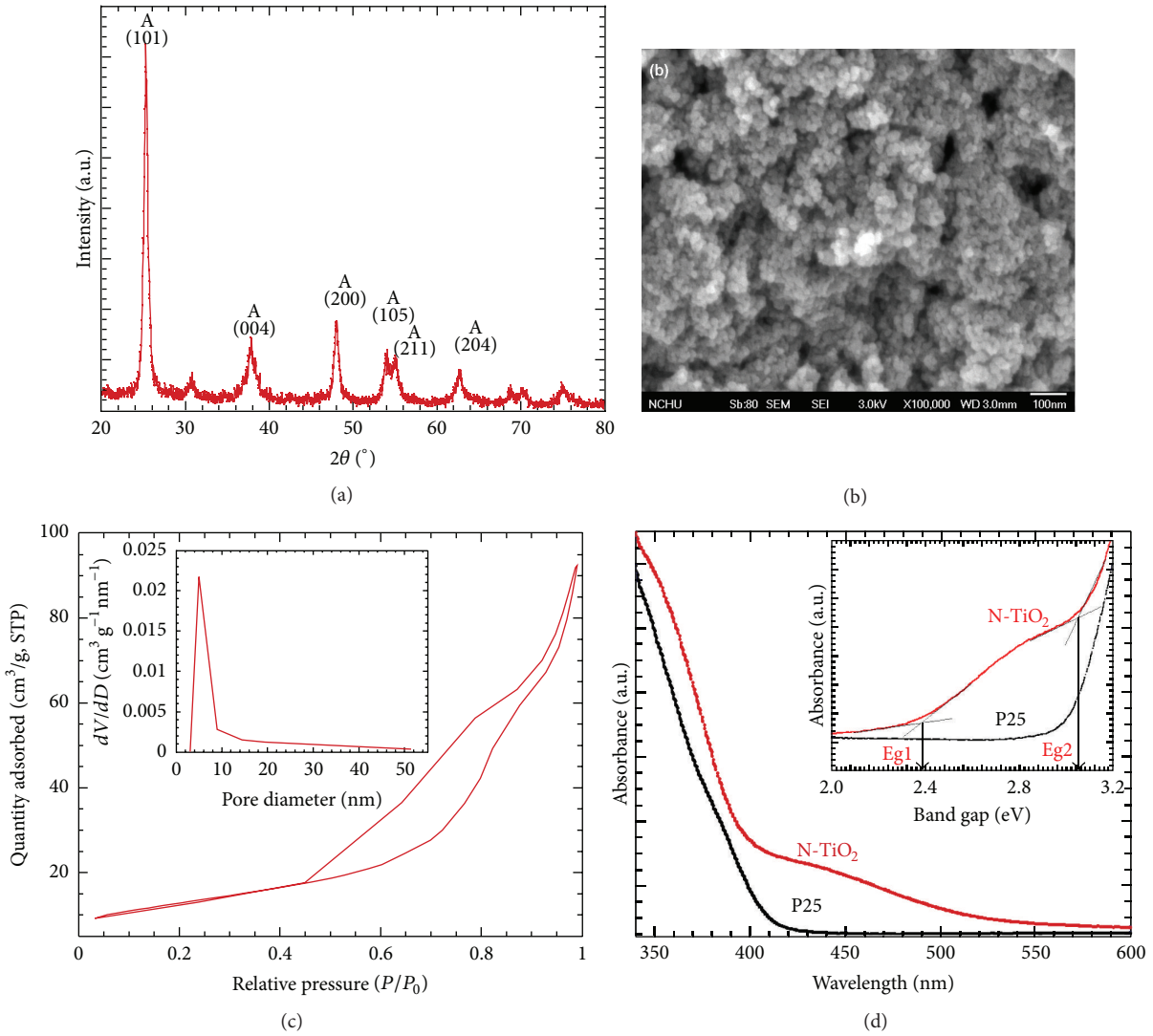

FIGURE 1: Characteristic of N-TiO_2 using (a) XRD, (b) SEM, (c), BET, and (d) UV-vis.

the converted acetaldehyde was mineralized to CO_2. Hence, the importance of the adsorption and photooxidation kinetics is investigated under the following experimental conditions.

3.2. Adsorption Kinetics

3.2.1. Effect of Reaction Temperature in Dark Condition. Temperature plays a crucial role in adsorption process. Figure 3 shows the extent of acetaldehyde adsorption as a function of contact time and temperature in the dark condition. It was observed that the amount of acetaldehyde adsorbed progressively increased with time and temperature. Equilibrium was achieved in 5 hr for a temperature higher than 5°C. In viewing all these kinetic curves, two phases were observed: (i) the first phase, where a rapid adsorption appeared within 1 hr contact time; (ii) the second phase, where a progressive adsorption occurred thereafter. In the fast adsorption phase, approximately 80% of acetaldehyde was removed. The subsequent slow adsorption stage was mainly caused by external active sites already being occupied by acetaldehyde, as well as by the slow diffusion of acetaldehyde into the pore spaces of N-TiO_2. In general, adsorption involves a multistep process where the rate of adsorption is limited by intraparticle diffusion.

The kinetic data was analyzed using PSO. The fittings of PSO to the kinetic data were presented as solid line in Figure 3. Table 2 summarizes the amount of acetaldehyde adsorbed onto N-TiO_2 sample at different temperatures and the corresponding fitting parameters of PSO model. Overall, the kinetic data correlate well with PSO models as judged from the high coefficient of determination values ($R^2 > 0.95$). The rate constant increased from 0.164 to 0.308 g/μmol/hr as temperature increased from 5 to 35°C. Thus, it was confirmed that an increase in temperature results in an increase in the adsorption rate. An increase in temperature may increase the driving force of diffusion across the external boundary layer and increase the rate of diffusion within the pores.

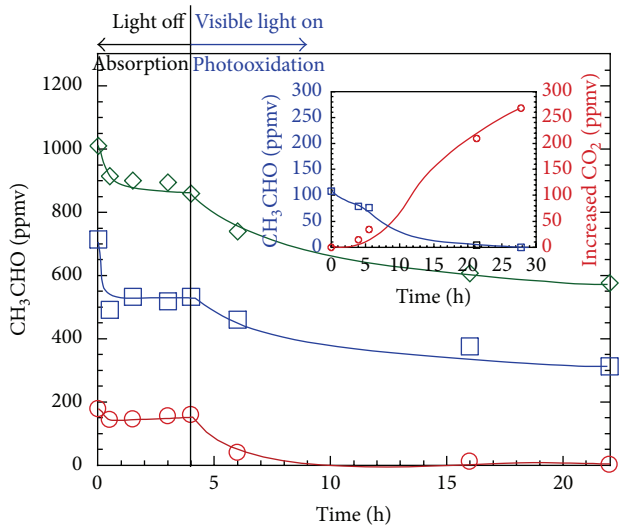

FIGURE 2: Adsorption and photooxidation of acetaldehyde onto the N-TiO_2 in the absence of light (dark) and under visible-light irradiation (light). Experimental conditions: [CH_3CHO] = 176–1010 ppmv and temperature = 25°C.

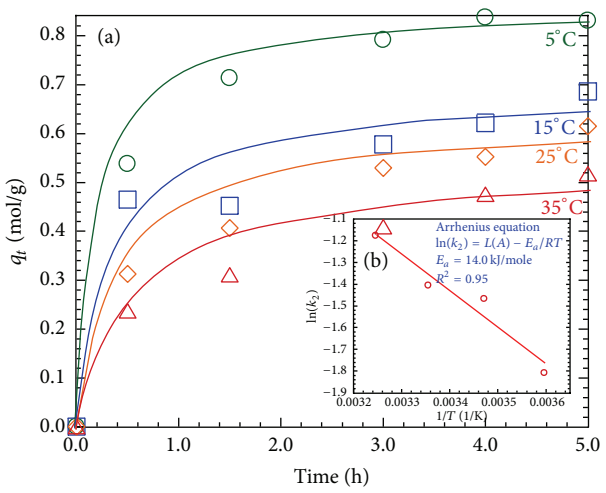

FIGURE 3: (a) The fitting of pseudo-second-order kinetic plots for the adsorption of acetaldehyde onto N-TiO_2 at various temperatures; the solid lines are the best fittings of PSO to the kinetic data. (b) Arrhenius equation plot for the adsorption of acetaldehyde onto N-TiO_2. Experimental conditions: $[CH_3CHO]_i$ = 176–1010 ppmv.

Consequently, more acetaldehyde easily enters the interior pore of N-TiO_2. The rate constants, k_2, listed in Table 2 can be related to temperature by Arrhenius equation and were used to determine the activation energy (E_a) of this adsorption process. From the Arrhenius plot of $\ln k_2$ versus $1/T$ (graph inset of Figure 3), an E_a of 14 kJ/mol was determined for the adsorption system. Normally a diffusion-controlled process has an E_a value lower than 42 kJ/mol [24]. The obtained E_a value is 14.0 kJ/mol, which indicates the adsorption of acetaldehyde that occurred during the diffusion control process [25].

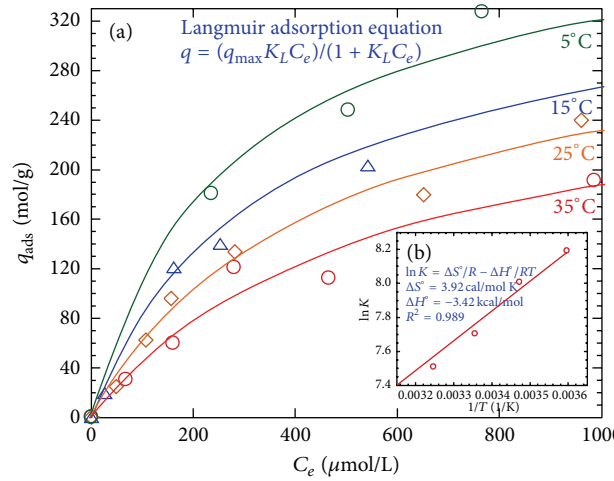

FIGURE 4: (a) Adsorption isotherms of acetaldehyde adsorption on N-TiO_2 at various temperatures. Solid lines are the best fit of Langmuir isotherm. (b) van't Hoff plot for the adsorption of acetaldehyde onto N-TiO_2.

3.2.2. Adsorption Isotherms. Figure 4 shows that the magnitude of acetaldehyde adsorption is proportional to temperature, and the results were fitted to the Langmuir isotherm model (equation (6)). Table 3 lists the Langmuir constants (i.e., q_{max} and K_L). The high coefficient of determination values confirms that the equilibrium data could be well represented by the Langmuir isotherm. The changes in the free energy (ΔG°), enthalpy (ΔH°), and entropy (ΔS°) in the adsorption reaction system were calculated from the van't Hoff plot (graph inset of Figure 4) and are listed in Table 3. The negative value of ΔH° (−3.42 kJ/mol) indicates that the adsorption mechanism is exothermic in nature and that it was a diffusion-controlled process [26]. Moreover, the small value of ΔH° implies weak bonding between acetaldehyde and the N-TiO_2 surface. The negative value of ΔG° and the positive value of ΔS° (3.92 cal/K/mol) indicate that the adsorption of acetaldehyde onto N-TiO_2 was a spontaneous process. The positive value of ΔS° in this study suggests increased randomness at the gas-solid interface with some structural changes in the adsorbate and the adsorbent [27, 28]. In other words, a dissociative adsorption of acetaldehyde occurred possibly on the N-TiO_2 surface during adsorption. But the low value of ΔS° may imply that no remarkable change in entropy occurred during the adsorption of acetaldehyde onto N-TiO_2. Normally, adsorption of gases causes a decrease in entropy owing to an orderly arrangement of the gas molecules on a surface. A slight increase in the ΔG° values from −4.60 to −4.53 kcal/mol with a decrease in temperature from 35 to 5°C indicated that the adsorption process was more favorable and spontaneous at low temperatures.

3.3. Photooxidation Kinetics

3.3.1. Effect of Acetaldehyde Concentration. The influence of various acetaldehyde concentrations on the rate of acetaldehyde photooxidation is shown in Figure 5, and the results

Table 2: Predicted constants of pseudo-second-order kinetic model for the adsorption of acetaldehyde onto N-TiO_2 at various temperatures.

Temperature (°C)	Pseudo-second-order model			Activation energy
	q_e (μmol/g)	k_2 (g/μmol/hr)	R^2	E_a (kJ/mol)
5	0.860	0.164	0.996	14.0
15	0.687	0.230	0.976	
25	0.630	0.245	0.977	
35	0.540	0.308	0.957	

Table 3: Thermodynamic parameters for the adsorption of acetaldehyde onto N-TiO_2 at various temperatures.

Temperature (°C)	q_{max} (μmol/g)	K_L (L/mol)	R^2	$\Delta G°$ (kcal/mol)	$\Delta H°$ (kcal/mol)	$\Delta S°$ (cal/K/mol)
5	196	0.0017	0.998	−4.53	−3.42	3.92
15	290	0.0018	0.979	−4.59		
25	336	0.0022	0.992	−4.57		
35	444	0.0036	0.982	−4.60		

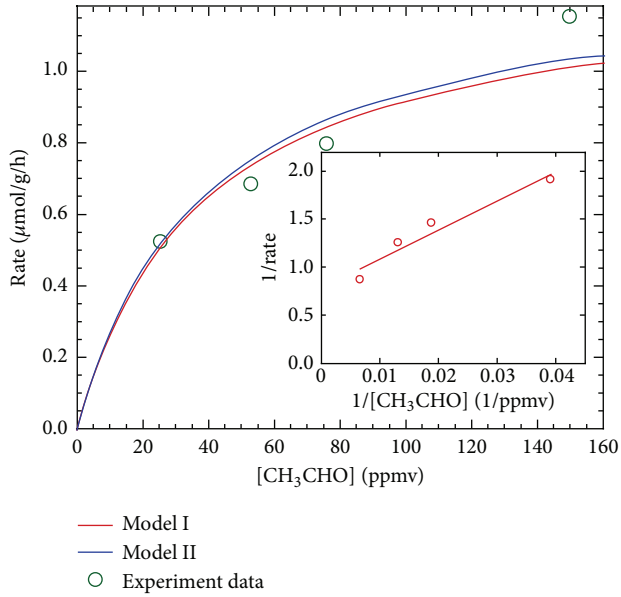

Figure 5: The effect of acetaldehyde concentration on the photocatalytic reaction. Experimental conditions: temperature = 25°C, I = 1.01 mW/cm^2.

correlated well with the L-H rate equation. Increasing the acetaldehyde concentration increases the concentration gradient between the bulk phase and the N-TiO_2 surface where the adsorption of the reactant becomes the rate-controlling step. Thus, the higher the acetaldehyde concentration, the faster the reaction rate. According to the L-H model, the rate of the reactant molecular reaction is proportional to the fraction of surface covered by the reactants. Light intensity and temperature were held constant to determine the rate constant (k) (model I in Table 1). If the L-H form is valid, a plot of reciprocal of the degradation rate (1/rate) versus reciprocal of the initial acetaldehyde concentration will be linear. The graph inset of Figure 5 shows the corresponding plot of 1/rate versus 1/[CH_3CHO] with good linearity. The red circles in Figure 5 represent a good fit of the experimental data to model I. It is clear that the L–H equation applied to one type of adsorption site which describes the initial acetaldehyde concentration dependencies satisfactorily. The values for k and K_a, generated by model fitting of the experimental data for a reaction temperature of 25°C, were 1.2666 μmol/cm^2 and 0.0263 ppmv^{-1}, respectively.

3.3.2. Effect of Visible-Light Intensity. The N-TiO_2 absorbs light with a threshold wavelength that is enough to provide energy to overcome the band gap between the valence band and the conduction band. For N-TiO_2, the wavelength of the visible light greater than 400 nm can provide enough energy to overcome the band gap (2.8 eV). At enough activation energy, the electrons will transfer between valence band and conduction band to form electron-hole pairs on the catalyst surface. The electron-hole pairs can trigger the photocatalytic oxidation reactions. Figure 6 depicts the effect of light intensity on the reaction rate of acetaldehyde. The effect of light intensity was examined under the reactant gas stream of 161 ppmv CH_3CHO at 25°C. The light intensity used in this experiment was in the range of 0.4–3 mW/cm^2. The reaction rates increased with increasing the light intensity, which can generate more photons and electron-hole pairs in the following series of free-radical reactions. The reaction rate constant is a function of light intensity according to a reported relationship [6]. By substituting the above relationship in model I under constant initial concentration of acetaldehyde, the rate expression should be

$$r = k'' I^{\alpha} \quad k'' = k' \frac{K_a C_a}{1 + K_a C_a}. \tag{8}$$

By plotting log(r) versus log(I) (graph inset of Figure 6), a straight line with a slope (α) of 0.111 and intercept (log k'') of 0.1112 is obtained and then the rate constant (k') is 1.2918 μmol/cm^2/hr/(mW/cm^2)$^{0.1112}$. The effect of light intensity on the photooxidation reaction was similar to that reported previously [29]. Photocatalytic reactors can be operated in two regimes with respect to light intensity: a first-order regime where the electron-hole pairs are consumed more rapidly by chemical reactions than by recombination,

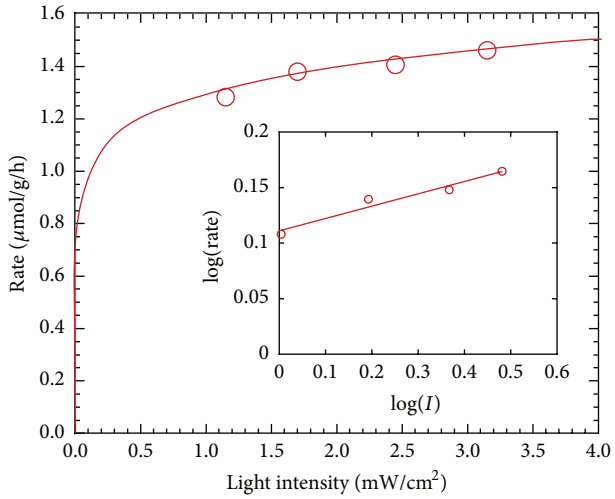

Figure 6: The effect of photon flux on the photocatalytic reaction. Experimental conditions: [CH_3CHO] = 161 ppmv and temperature = 25°C.

and a 0.5-order regime where the recombination rate dominates [30]. The present result was consistent with the above phenomenon indicating that the dominant mechanism is the electron-hole pair recombination reaction.

To include explicit environmental condition dependence in the rate equation, the following assumptions were made: the Langmuir adsorption constants for monolayer adsorption on a homogeneous surface can be applied on predicting the photooxidation rate of the N-TiO_2, and the rate constant (k) follows Arrhenius temperature dependence. With these assumptions, a photooxidation rate of the N-TiO_2 is given by model II (Table 1). The constants of model II are summarized in Table 4 and the values calculated are in good agreement with the experimental data, as shown by blue squares in Figure 5. The model II was used to identify the range of two key parameters (i.e., acetaldehyde concentrations and visible-light intensity) that would lead to an enhanced acetaldehyde oxidation rate. As evident from Figure 7, when a photocatalytic device with the N-TiO_2 catalyst operated at a maximum acetaldehyde concentration of approximately 250 ppmv, the oxidation rate would approach a constant value. Specifically, oxidation rate of the N-TiO_2 photocatalyst increased with elevated acetaldehyde concentration and visible-light intensity.

3.4. Acetaldehyde Removal Mechanism in Indoor Environment Using the N-TiO_2. To illustrate clearly the acetaldehyde removal mechanism of N-TiO_2 under the indoor environment, a conceptual reaction scheme of the photocatalytic oxidation of the acetaldehyde using N-TiO_2 nanomaterial is proposed (Figure 8). In the dark indoor environment, such as nighttime, the acetaldehyde pollutant will diffuse from air phase to the surface of N-TiO_2 catalyst. The acetaldehyde would be absorbed onto N-TiO_2 particles, and decreased temperature results in an increase in the adsorption rate. When the visible light was turned on, the N-TiO_2 catalyst had shown a stronger absorption in the visible-light region of 400–500 nm wavelength possibly due to the fact that

Table 4: Langmuir-Hinshelwood parameters for models I and II.

Parameter	Unit	Type of kinetic model	
		I	II
k	μmol/h	1.2666	—
K_a	1/ppmv	0.0263	0.0263
α	—	—	0.1110
k'	μmol/cm²/hr/(mW/cm²)$^{0.1112}$	—	1.2918

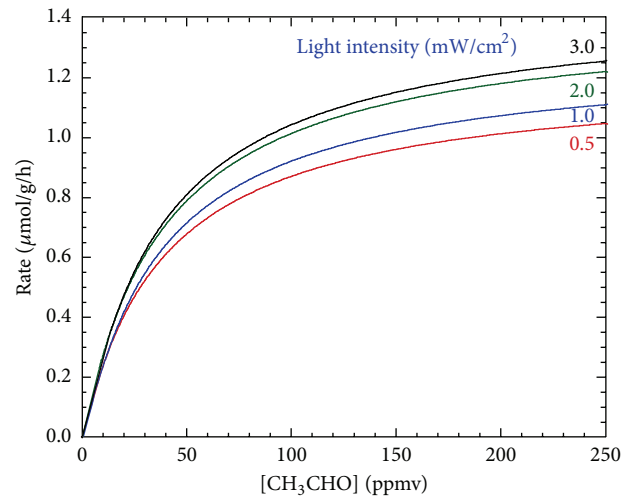

Figure 7: Predicted oxidation rate dependence on acetaldehyde concentration and light intensity (model II).

the band gap was narrowed by mixing of nitrogen 2p states with O 2p states on the top of the valence band or a creation of N-induced midgap level [31, 32]; the absorption at wavelength above 500 nm is ascribed to oxygen vacancy. The excited electron (e^-) was generated from N-TiO_2 and transferred to contact with acetaldehyde. At the same time, the remaining holes also migrate outward to form reactive species and react with acetaldehyde in indoor air. Therefore, the acetaldehyde was photooxidized by N-TiO_2 and the photooxidation rate increased with elevated acetaldehyde concentration, but it was less sensitive to the changes of visible-light intensity.

4. Conclusions

Indoor acetaldehyde pollutant is harmful for human health. It is highly potential that the home appliances with visible-light-responsive TiO_2 photocatalyst, such as N-TiO_2, can be used to remove the acetaldehyde pollutant in future. In practical application, using the photocatalyst to remove the indoor acetaldehyde involves an absorption and photooxidation process in dark and visible-light irradiation, respectively. The key parameters of the removal of the acetaldehyde pollutant using N-TiO_2 photocatalyst under the practical indoor environment conditions were investigated. The kinetics and mechanism of the removal of the acetaldehyde pollutant using N-TiO_2 photocatalyst will be useful for applicability of these home appliances.

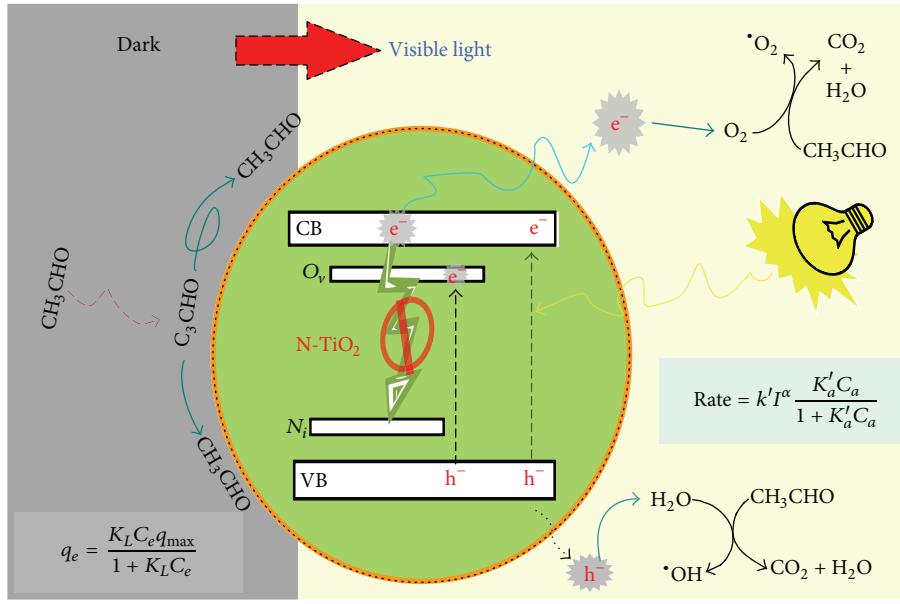

FIGURE 8: Conceptual reaction mechanism of N-TiO_2 under an indoor environment for acetaldehyde removal.

An increase in temperature results in a decrease in the acetaldehyde adsorption rate. The adsorption reaction was a spontaneous and exothermic process. The reaction rate of acetaldehyde photooxidation increased with increasing acetaldehyde concentration and light intensity. The kinetic studies confirm that the reaction rate is successfully predicted using the L–H kinetic model. A reaction mechanism scheme for removal process of acetaldehyde using N-TiO_2 under illumination of visible light was proposed. In conclusion, the prepared N-TiO_2 photocatalyst has a high ability to absorb acetaldehyde in the dark conditions and has a significantly high photocatalytic activity under visible-light irradiation.

Competing Interests

The authors declare that there is no conflict of interests regarding the publication of this paper.

Acknowledgments

This study was supported by the Ministry of Science and Technology of ROC (Grant nos. NSC 102-2120-M-005-002 and NSC 102-2221-E-005-001-MY3) and the Ministry of Economic Affairs of ROC (Grant no. 101/102/103-EC-17-A-21-S1-229).

References

[1] E. Obuchi, T. Sakamoto, K. Nakano, and F. Shiraishi, "Photocatalytic decomposition of acetaldehyde over TiO_2/SiO_2 catalyst," *Chemical Engineering Science*, vol. 54, no. 10, pp. 1525–1530, 1999.

[2] J.-Y. Rau, H.-H. Tseng, M.-D. Lin et al., "Characterization of polycyclic aromatic hydrocarbon emission from open burning of joss paper," *Atmospheric Environment*, vol. 42, no. 8, pp. 1692–1701, 2008.

[3] Z. Jiang, M. Chen, J. Shi, J. Yuan, and W. Shangguan, "Catalysis removal of indoor volatile organic compounds in room temperature: from photocatalysis to active species assistance catalysis," *Catalysis Surveys from Asia*, vol. 19, no. 1, pp. 1–16, 2015.

[4] Z. Zhang and J. Gamage, "Applications of photocatalytic disinfection," *International Journal of Photoenergy*, vol. 2010, Article ID 764870, 11 pages, 2010.

[5] B. Hauchecorne, D. Terrens, S. Verbruggen et al., "Elucidating the photocatalytic degradation pathway of acetaldehyde: an FTIR in situ study under atmospheric conditions," *Applied Catalysis B: Environmental*, vol. 106, no. 3-4, pp. 630–638, 2011.

[6] J. Zhao and X. Yang, "Photocatalytic oxidation for indoor air purification: a literature review," *Building and Environment*, vol. 38, no. 5, pp. 645–654, 2003.

[7] L. Zhong, F. Haghighat, C.-S. Lee, and N. Lakdawala, "Performance of ultraviolet photocatalytic oxidation for indoor air applications: systematic experimental evaluation," *Journal of Hazardous Materials*, vol. 261, pp. 130–138, 2013.

[8] R. Asahi, T. Morikawa, H. Irie, and T. Ohwaki, "Nitrogen-doped titanium dioxide as visible-light-sensitive photocatalyst: designs, developments, and prospects," *Chemical Reviews*, vol. 114, no. 19, pp. 9824–9852, 2014.

[9] R. Amadelli, L. Samiolo, A. Maldotti, A. Molinari, M. Valigi, and D. Gazzoli, "Preparation, characterisation, and photocatalytic behaviour of Co-TiO_2 with visible light response," *International Journal of Photoenergy*, vol. 2008, Article ID 853753, 9 pages, 2008.

[10] G. Shang, H. Fu, S. Yang, and T. Xu, "Mechanistic study of visible-light-induced photodegradation of 4-chlorophenol by $TiO_{2-x}N_x$ with low nitrogen concentration," *International Journal of Photoenergy*, vol. 2012, Article ID 759306, 9 pages, 2012.

[11] Y. Zhang, H. Wu, and P. Liu, "Enhanced transformation of atrazine by high efficient visible light-driven N, S-codoped TiO_2

nanowires photocatalysts," *International Journal of Photoenergy*, vol. 2014, Article ID 425836, 8 pages, 2014.

[12] H. Chen, Z. Xie, X. Jin et al., "TiO_2 and N-doped TiO_2 induced photocatalytic inactivation of *Staphylococcus aureus* under 405 nm LED blue light irradiation," *International Journal of Photoenergy*, vol. 2012, Article ID 848401, 5 pages, 2012.

[13] Y.-T. Lin, C.-H. Weng, H.-J. Hsu, Y.-H. Lin, and C.-C. Shiesh, "The synergistic effect of nitrogen dopant and calcination temperature on the visible-light-induced photoactivity of N-doped TiO_2," *International Journal of Photoenergy*, vol. 2013, Article ID 268723, 13 pages, 2013.

[14] Y.-H. Lin, C.-H. Weng, A. L. Srivastav, Y.-T. Lin, and J.-H. Tzeng, "Facile synthesis and characterization of N-Doped TiO_2 photocatalyst and its visible-light activity for photo-oxidation of ethylene," *Journal of Nanomaterials*, vol. 2015, Article ID 807394, 10 pages, 2015.

[15] I.-C. Kang, Q. Zhang, S. Yin, T. Sato, and F. Saito, "Improvement in photocatalytic activity of TiO_2 under visible irradiation through addition of N-TiO_2," *Environmental Science & Technology*, vol. 42, no. 10, pp. 3622–3626, 2008.

[16] Y.-T. Lin, C.-H. Weng, Y.-H. Lin, C.-C. Shiesh, and F.-Y. Chen, "Effect of C content and calcination temperature on the photocatalytic activity of C-doped TiO_2 catalyst," *Separation and Purification Technology*, vol. 116, pp. 114–123, 2013.

[17] Y.-T. Lin, C.-H. Weng, and F.-Y. Chen, "Key operating parameters affecting photocatalytic activity of visible-light-induced C-doped TiO_2 catalyst for ethylene oxidation," *Chemical Engineering Journal*, vol. 248, pp. 175–183, 2014.

[18] N. Bao, Y. Li, Z. Wei, G. Yin, and J. Niu, "Adsorption of dyes on hierarchical mesoporous TiO_2 fibers and its enhanced photocatalytic properties," *The Journal of Physical Chemistry C*, vol. 115, no. 13, pp. 5708–5719, 2011.

[19] F. Venditti, F. Cuomo, A. Ceglie, P. Avino, M. V. Russo, and F. Lopez, "Visible light caffeic acid degradation by carbon-doped titanium dioxide," *Langmuir*, vol. 31, no. 12, pp. 3627–3634, 2015.

[20] S. Sato, R. Nakamura, and S. Abe, "Visible-light sensitization of TiO_2 photocatalysts by wet-method N doping," *Applied Catalysis A: General*, vol. 284, no. 1-2, pp. 131–137, 2005.

[21] N. D. Abazović, A. Montone, L. Mirenghi, I. A. Janković, and M. I. Čomor, "TiO_2 doped with Nitrogen: synthesis and characterization," *Journal of Nanoscience and Nanotechnology*, vol. 8, no. 2, pp. 613–618, 2008.

[22] I. Nakamura, N. Negishi, S. Kutsuna, T. Ihara, S. Sugihara, and K. Takeuchi, "Role of oxygen vacancy in the plasma-treated TiO_2 photocatalyst with visible light activity for NO removal," *Journal of Molecular Catalysis A: Chemical*, vol. 161, no. 1-2, pp. 205–212, 2000.

[23] T. Ihara, M. Miyoshi, Y. Iriyama, O. Matsumoto, and S. Sugihara, "Visible-light-active titanium oxide photocatalyst realized by an oxygen-deficient structure and by nitrogen doping," *Applied Catalysis B: Environmental*, vol. 42, no. 4, pp. 403–409, 2003.

[24] X. S. Wang, Y. P. Tang, and S. R. Tao, "Kinetics, equilibrium and thermodynamic study on removal of Cr (VI) from aqueous solutions using low-cost adsorbent Alligator weed," *Chemical Engineering Journal*, vol. 148, no. 2-3, pp. 217–225, 2009.

[25] S. Tunali, A. S. Özcan, A. Özcan, and T. Gedikbey, "Kinetics and equilibrium studies for the adsorption of Acid Red 57 from aqueous solutions onto calcined-alunite," *Journal of Hazardous Materials*, vol. 135, no. 1–3, pp. 141–148, 2006.

[26] M. Hema and S. Arivoli, "Adsorption kinetics and thermodynamics of malachite green dye unto acid activated low cost carbon," *Journal of Applied Sciences and Environmental Management*, vol. 12, no. 1, 2008.

[27] I. Mobasherpour, E. Salahi, and M. Ebrahimi, "Thermodynamics and kinetics of adsorption of Cu(II) from aqueous solutions onto multi-walled carbon nanotubes," *Journal of Saudi Chemical Society*, vol. 18, no. 6, pp. 792–801, 2014.

[28] P. Saha and S. Chowdhury, *Insight into Adsorption Thermodynamics*, INTECH Open Access Publisher, 2011.

[29] G. Vincent, P. M. Marquaire, and O. Zahraa, "Photocatalytic degradation of gaseous 1-propanol using an annular reactor: kinetic modelling and pathways," *Journal of Hazardous Materials*, vol. 161, no. 2-3, pp. 1173–1181, 2009.

[30] W. A. Jacoby, D. M. Blake, R. D. Noble, and C. A. Koval, "Kinetics of the oxidation of trichloroethylene in air via heterogeneous photocatalysis," *Journal of Catalysis*, vol. 157, no. 1, pp. 87–96, 1995.

[31] M. Batzill, E. H. Morales, and U. Diebold, "Influence of nitrogen doping on the defect formation and surface properties of TiO_2 rutile and anatase," *Physical Review Letters*, vol. 96, no. 2, Article ID 026103, 2006.

[32] H. Chen, A. Nambu, W. Wen et al., "Reaction of NH_3 with titania: N-doping of the oxide and TiN formation," *The Journal of Physical Chemistry C*, vol. 111, no. 3, pp. 1366–1372, 2007.